Journal of Cranio-Maxillo-Facial Surgery 48 (2020) 574–581

Contents lists available at ScienceDirect

Journal of Cranio-Maxillo-Facial Surgery

journal homepage: www.jcmfs.com

Reliability of orbital volume measurements based on computed tomography segmentation: Validation of different algorithms in orbital trauma patients

Yurii Chepurnyi [a, *], Denys Chernohorskyi [a], Danylo Prykhodko [b], Arto Poutala [c], Andriy Kopchak [a]

[a] Department of Stomatology, Bogomolets National Medical University, T. Shevchenko Blvd., 13, 01601, Kyiv, Ukraine
[b] "Imatek Medical Co", Prosp, Peremogy, 123, 03179, Kyiv, Ukraine
[c] "Disior Ltd", FI27875878, Terkko Health Hub, Haartmaninkatu 4, 00290, Helsinki, Finland

ARTICLE INFO

Article history:
Paper received 17 October 2019
Accepted 19 March 2020
Available online 29 March 2020

Keywords:
Orbital volume
Semi-automated segmentation
Automated segmentation
Orbital reconstruction

ABSTRACT

Purpose: To compare the most common methods of segmentation for evaluation of the bony orbit in orbital trauma patients.
Materials and methods: Computed tomography scans (before and after treatment) from 15 patients with unilateral blowout fractures and who underwent orbital reconstructions were randomly selected for this study. Orbital volume measurements, volume difference measurements, prolapsed soft tissue volumes, and bony defect areas were made using manual, semi-automated, and automated segmentation methods.
Results: Volume difference values between intact and damaged orbits after surgery using the manual mode were 0.5 ± 0.3 cm^3, 0.5 ± 0.4 cm^3 applying semi-automated method, and 0.76 ± 0.5 cm^3, determined by automated segmentation ($p = 0.216$); the mean volumes (MVs) for prolapsed tissues were 3.0 ± 1.9 cm^3, 3.0 ± 2.3 cm^3, and 2.8 ± 3.9 cm^3 ($p = 0.152$); and orbital wall defect areas were 4.7 ± 2.8 cm^2, 4.75 ± 3.1 cm^2, and 4.9 ± 3.3 cm^2 ($p = 0.674$), respectively.
Conclusions: The analyzed segmentation methods had the same accuracy in evaluation of volume differences between two orbits of the same patient, defect areas, and prolapsed soft tissue volumes but not in absolute values of the orbital volume due to the existing diversity in determination of anterior closing. The automated method is recommended for common clinical cases, as it is less time-consuming with high precision and reproducibility.

1. Introduction

The bony orbit is a complex anatomical structure, with major functional and clinical significance. Its volume, shape, and integrity can be compromised in patients with midfacial trauma, congenital pathologies, tumours, and postsurgical defects (Comerci et al., 2013; Wagner et al., 2016; Wilde et al., 2019). Accurate three-dimensional (3D) reconstruction of its walls, with restoration to its original shape and volume in these cases, is crucial for functional and cosmetic rehabilitation, complication prophylaxis, and long-term prognosis (Dubois et al., 2014; Kärkkäinen et al., 2018). Precise *in vivo* orbital assessments and volume measurements are important components for diagnostics, treatment and operation planning, and rehabilitation of patients with orbital pathologies (Bijlsma and Mourits, 2006; Scolozzi and Jaques, 2008; Noser et al., 2018; Essig et al., 2013).

Segmentation of computed tomography (CT) data, and generation of precise virtual 3D models of the bony orbit and its soft tissue content, has made it possible to estimate the geometry and volume of the affected orbit *in vivo* (Essig et al., 2013; Strong et al., 2013; Choi and Kang, 2017; Sozzi et al., 2018). A number of studies have compared direct measurements of orbital volume with CT-segmentation measurements on cadaveric skulls and found

* Corresponding author. Department of Stomatology, Bogomolets National Medical University, T. Shevchenko blvd, 13, 01601, Kyiv, Ukraine.
E-mail address: 80667788837@ukr.net (Y. Chepurnyi).

https://doi.org/10.1016/j.jcms.2020.03.007
1010-5182/

discrepancies of 4–8%, or more between the two methods (Cooper, 1985; Osaki et al., 2013; Diaconu et al., 2017).

Several algorithms for segmentation are currently available, and both semi-automated and automated versions have been developed over the past few decades (Wagner et al,. 2016; Galibourg et al., 2018; Queiroz et al., 2017; Tang et al., 2018). Clinical applicability of these algorithms depends predominantly on how fast, accurate, and reproducible they are (Scolozzi and Jaques, 2008; Lukats et al., 2013; Metzger et al., 2013; Jansen et al., 2016; Wagner et al., 2016; Choi and Kang, 2017).

Despite significant improvements in both CT quality and these algorithms, the reliability of digital orbital volume measurements is still uncertain. According to the literature, orbital volume estimates are still highly dependent on the algorithm used, the type and quality of CT datasets, and the evaluator's skill and experience (Hu et al., 2012; Essig et al., 2013; Jansen et al., 2016; Wagner et al., 2016; Fu et al., 2017). The main problems reported by these studies (making segmentation more complicated and less predictable) were the very thin boundaries of the bony orbit, and the difficulty determining its anterior and posterior borders. The anterior surface of the orbit, with a perimeter shaped by orbital margins, most closely resembles a hyperbolic paraboloid (a saddle-like surface). The anterior part of the orbit has the widest diameter and is therefore responsible for the greatest deviations in volume measurements, even with small differences in diameter estimations (Essig et al., 2013; Osaki et al., 2013; Strong et al., 2013; Wagner et al., 2016). Thus it is still a significant challenge to define and adequately represent the anterior border of the orbit using existing software.

Despite numerous publications on the virtual evaluation of orbital volume using different software and different methods of segmentation, only a few have compared manual, semi-automated, and fully automated segmentation (Paiement et al., 2014; Jansen et al., 2016; Wagner et al., 2016). However, all of these studies investigated only healthy orbits, so their results cannot be directly applied to orbital trauma cases. For orbital injuries, evaluations focus mainly on measuring orbital volumes before and after surgery using in the same specified software environment. This makes comparing results across studies difficult, especially concerning the efficacy of orbital wall reconstructions, and any decision-making and diagnostics based on orbital volumetry.

The goals of the present study were to compare the most common methods of orbital volume measurement in orbital trauma patients, and to make recommendations for application of these orbital segmentation methods in certain clinical cases.

2. Materials and methods

This study met the requirements of the Declaration of Helsinki and was approved by the Ethics Committee of the Bohomolets National Medical University (No 126, November 13, 2019). All personal data (CT) were used anonymously, which waived the need for informed consent. CT scans of 15 patients who had unilateral blowout fractures of the orbit and who underwent orbital reconstructions with patient-specific implants (PSIs) at Kyiv Regional Centre for Maxillofacial Surgery and Stomatology were randomly selected for the study. Inclusion criteria were as follows: a unilateral blowout fracture with unaffected orbital margins, surgical treatment with a PSI no later than 1 month after trauma, and good quality CT data available before and after surgery, with both slice thickness and slice increment $\leq$0.5 mm. Exclusions based on data acquired using different CT trauma protocols were intentionally avoided.

Of 15 patients included in the study, 11 were male; the mean age was 36.4 $\pm$ 7.8 years. Evaluations of affected and unaffected orbits based on acquired CT data were performed for diagnostics, treatment planning, PSI design, and estimations of unilateral orbital reconstructions. Orbital volumetry was conducted retrospectively for both orbits in all patients, before and after treatment, by two different observers, each with more than 5 years of clinical experience using manual, semi-automated and automated segmentation methods.

To check the reproducibility of the results obtained by each method, volume measurements of intact orbits before and after surgery, and injured orbits before and after orbital reconstruction, were performed twice, by two independent examiners, for each method of segmentation. This study's most important criteria evaluated for orbital trauma surgery were the volumes of prolapsed orbital soft tissues, and area measurements of the orbital wall bony defects.

2.1. Manual segmentation

In the present study, manual segmentation was performed using SimPlant software (Materialase, Leuven, Belgium) installed on a standard personal computer running Windows 7, with an Intel CORE I7 processor, and 16 GB of random access memory. The selected CT DICOM files were imported by the software, displayed as axial, coronal and sagittal plane images, and used to create threshold-based 3D reconstructions. A density interval appropriate for soft tissues was applied for segmentation with the use of a threshold function. Image masking was restricted to the region of interest (the orbit and surrounding tissues). Segmentation began from the anterior-most opening of the optic nerve foramen, at the level of the orbit's greatest anteroposterior length. Moving anteriorly, orbital volume was segmented by removing excessive mask volume, and tracing the orbital boundaries manually in each coronal slice. Area measurements of orbital wall defects with dislocated soft tissue were segmented according to tissue density. An anterior orbital plane mask was created by manually editing the excessive volume bounded by the perimeter of the orbital margins, and then a virtual model was automatically calculated (and volume determined) from the mask. For a volume measurement of the dislocated (prolapsed) soft orbital tissues, the mask was duplicated, and all intraorbital mask volume was removed (Fig. 1). After that removal, another virtual model was calculated from this new mask, and the volume was measured. At the end of the process, an additional mask was created based on bone density threshold. After

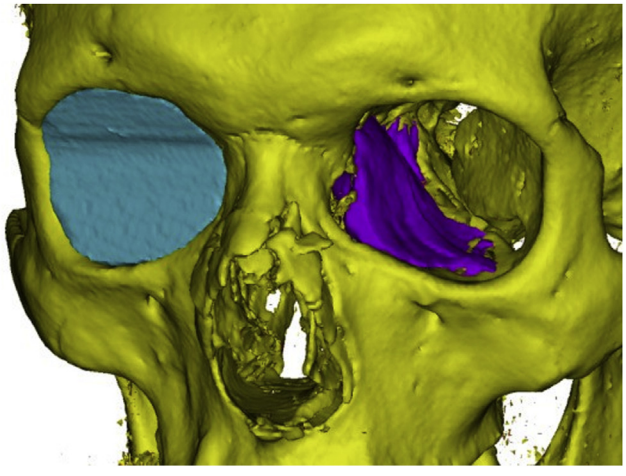

Fig. 1. Manually segmented virtual models of the orbit (SimPlant software): right orbit (blue), intact; left orbit, damaged (prolapsed volume is marked in violet).

generating the virtual models of the bony orbits, the wall defects caused by the blowout fractures were presented as ellipses, and their areas were measured. These area measurements roughly reproduced the areas of the orbital wall defects.

2.2. Semi-automated segmentation

Semi-automated segmentation was performed using D2P software (version 1.0.2.53, Simbionix Ltd/3D Systems Inc., Beit Golan, Israel). Imported DICOM files were visualized in axial, coronal, and sagittal planes using a threshold-based 3D reconstruction preview. In the software's multi-slice mode, intraorbital soft-tissue content on coronal slices (density range from −200 to 200 HU) was marked at the following levels: the anterior opening of the optic nerve channel; the posterior end of the inferior orbital fissure; the anterior end of the inferior orbital fissure; the lateral orbital margin; the middle of the orbital rim; and the anterior lacrimal crest. Next, a mask of the orbital soft tissue content was created by interpolation between the marked slices. Excessive volume in the anterior part of the mask was removed manually to achieve an anterior orbital plane bounded by the perimeter of the orbital margins. The orbital volume was automatically calculated while generating the virtual model (Fig. 2). Volume measurements for dislocated orbital soft tissues and area measurements of the bony defects were performed in the same manner described above for manual segmentation.

2.3. Automated segmentation

Automatic orbital segmentation was performed using Disior Orbital Analysis Software (Helsinki, Finland). DICOM data were imported by the software, which converted the image information into a voxel map, and created a 3D rendering of the craniofacial bone structure using a threshold-based method. After rendering, the evaluator marked a point roughly within each orbit (a so-called seed point). Exact seed point locations were not important for the software and did not affect the results. The software required an HU range for soft tissues (the default range was from −300 to 230 HU), and, when needed, this range was manually adjusted to match different image reconstructions. Finally, the evaluator confirmed to the software that the orbit indicated was fractured.

With these settings, the software segmented the orbits automatically, and no further interaction with the user was required. In particular, the anterior orbital opening was determined automatically, and was therefore user-independent, unless the predefined soft tissue HU range was altered (Fig. 3).

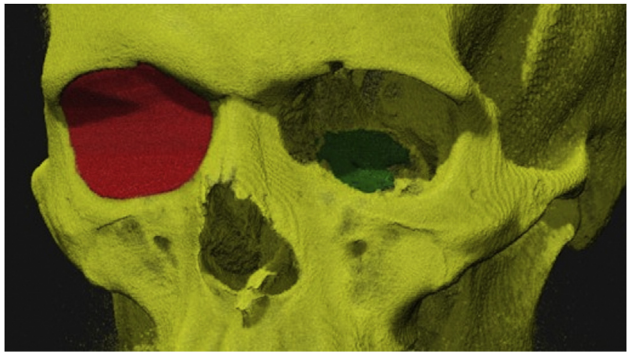

Fig. 2. Virtual models of the orbit, segmented in semi-automated mode (D2P software): right orbit, intact (red); left orbit, damaged (prolapsed volume is marked green).

For statistical analyses, IBM SPSS Statistics software (version 22, IBM, Armonk, NY, USA), was used with the level of significance set at $p < 0.05$. The Kolmogorov–Smirnov test was used to determine sample distribution. For variables with a normal (Gaussian) distribution, means ± standard deviations (SD) were used, and comparisons were made using paired Student *t* tests and analysis of variance (including repeated-measures analysis of variance). Comparisons between variables with non-Gaussian distribution were made using the Mann–Whitney *U* test, Kruskal-Wilcoxon signed rank test, Kruskal–Wallis *H* test, and Friedman test. These were used to compare the differences between parameters in the study groups. To test for interobserver and intraobserver agreement for all measurements, the intraclass correlation coefficient (ICC), and 95% confidence interval (CI) were measured for all segmentation methods.

3. Results

Measurements of orbital volume, pre- and postsurgery volume differences, prolapsed soft tissue volume, and bony defect areas were made in 15 patients before and after surgery. A total of 60 orbits were evaluated using manual, semi-automated, and automated modes of segmentation (Fig. 4).

3.1. Evaluation of the intact orbits

For manual segmentation, the mean volume (MV) of intact orbits was 25.6 ± 2.9 cm^3 before surgery and 25.6 ± 2.8 cm^3 after surgery ($t = 0.093$; $df = 14$, $p = 0.927$). The mean volume difference between the same pre- and postsurgery intact orbits was 0.5 ± 0.3 cm^3. Semi-automated segmentation of these intact orbits resulted in an MV of 26.3 ± 2.9 cm^3 before surgery and 26.4 ± 3.0 cm^3 after reconstruction, with a mean difference of 0.3 ± 0.2 cm^3 ($t = -1.085$; $df = 14$, $p = 0.296$). Measurements performed in automatic mode resulted in a MV before surgery of 28.0 ± 2.8 cm^3 and 27.9 ± 2.7 cm^3 after reconstruction, with a mean difference of 0.25 ± 0.15 cm^3 ($t = 1.802$; $df = 14$, $p = 0.093$). No significant differences were found between these single-segmentation methods for pre-and postsurgery volume differences ($F_2 = 3.696$, $p = 0.75$), with virtually the same variation seen for all three methods (Table 1).

3.2. Evaluation of damaged orbits

Manual segmentation MV was 29.4 ± 4.5 cm^3 before surgery and 25.6 ± 3.2 cm^3 after surgery. Semi-automated and automated volume evaluations resulted in mean orbital volumes of 29.9 ± 4.1 cm^3 and 30.8 ± 4.3 cm^3, respectively, before orbital reconstructions, and 26.7 ± 3.0 cm^3 and 27.6 ± 2.9 cm^3, respectively, after surgery ($F_1 = 1318$; $p < 0.001$) (Fig. 5). The volume changes of the damaged orbits after surgery, measured by all methods of segmentation, were virtually equal: manual −3.9 ± 2.2 cm^3; semi-automated −3.4 ± 1.6 cm^3; and automated −3.2 ± 3.1 cm^3 ($Fr = 1.6$; $df = 2$, $p = 0.449$) (Table 2).

Analysing the differences between intact and damaged orbital volumes measured using the three different software programs before surgery, these differences were 3.8 ± 2.6 cm^3 for the manual mode, 3.7 ± 2.2 cm^3 for the semi-automated mode, and 2.8 ± 2.9 cm^3 for the automated mode ($H = 5.6$; $df = 2$, $p = 0.061$). After surgery, these differences decreased to 0.5 ± 0.3 cm^3, 0.5 ± 0.4 cm^3, and 0.76 ± 0.5 cm^3, respectively ($H = 3.07$; $df = 2$, $p = 0.216$) (Table 3) (Fig. 6).

In these patients, the prolapsed tissue volumes measured by manual segmentation were 3.0 ± 1.9 cm^3. For the semi-automated

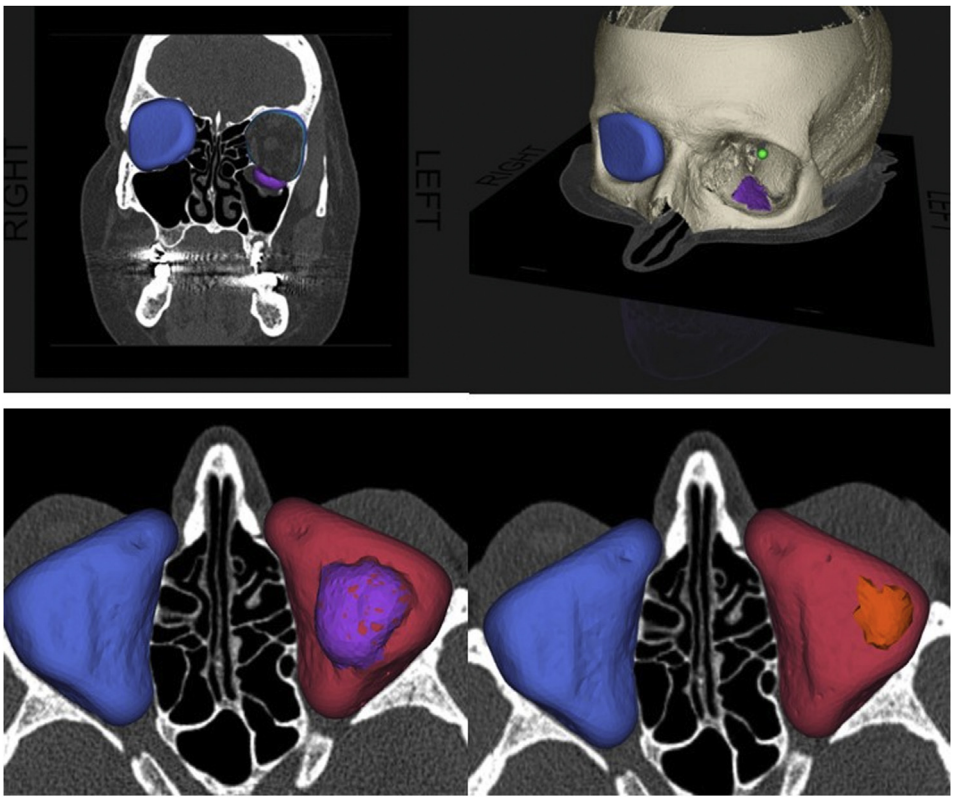

Fig. 3. Virtual models of the orbit segmented in automated mode (Disior software). A preoperative image (lower left) and a corresponding postoperative image (lower right). The intact right orbit is marked in blue and the damaged left orbit is in red. The prolapsed volume is marked in violet. A small overcorrection in the postoperative image is in orange.

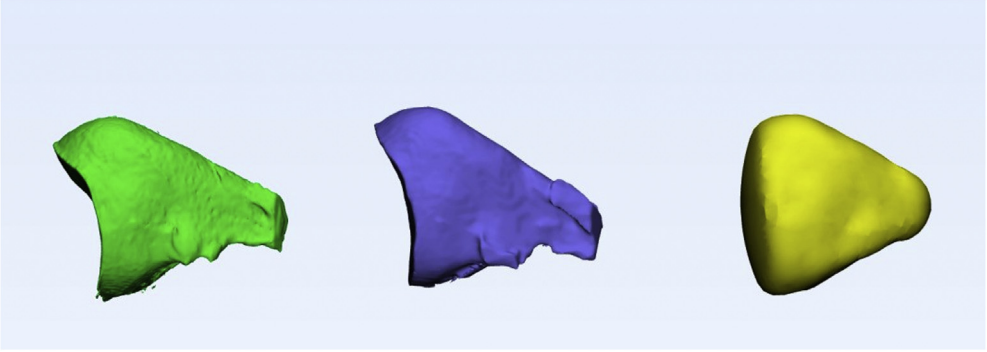

Fig. 4. Segmented orbital models: green, manual mode; violet, semi-automatic mode; yellow, automatic mode.

and automated modes, the values were 3.0 ± 2.3 cm^3 and 2.8 ± 3.9 cm^3, respectively (Fr = 3.736; df = 2; p = 0.152). All three software programs showed virtually equal values for orbital wall defect areas: 4.7 ± 2.8 cm^2, 4.75 ± 3.1 cm^2, and 4.9 ± 3.3 cm^2, respectively, with no significant differences (p = 0.674).

Table 1
Volume measurements of intact orbits.

Mode Mean volume (cm^3)	Manual	Semi-automatic	Automatic	p Value
Before surgery	25.6 ± 2.9	26.3 ± 2.9	28.0 ± 2.8	p < 0.001
After surgery	25.6 ± 2.8	26.4 ± 3.0	27.9 ± 2.7	p < 0.001
p Value	0.927	0.296	0.093	-

The intraobserver and interobserver ICCs for all modes of segmentation are shown in Table 4.

4. Discussion

Accurate 3D reconstruction of the bony orbit with restoration of its shape and volume is the main goal of orbital trauma surgery (Scolotzzi and Jaques, 2009; Noser et al., 2018; Essig et al., 2013). The precise evaluation of the location, size, and character of an orbital wall defect plays an important role in operation planning, the design of orbital implants, and prognosis of the surgical intervention (Regensburg et al., 2008; Noser et al., 2018; Essig et al., 2013; Choi and Kang, 2017).

The possibility for accurate *in vivo* measurements of orbital volume is associated with the development of high-resolution CT

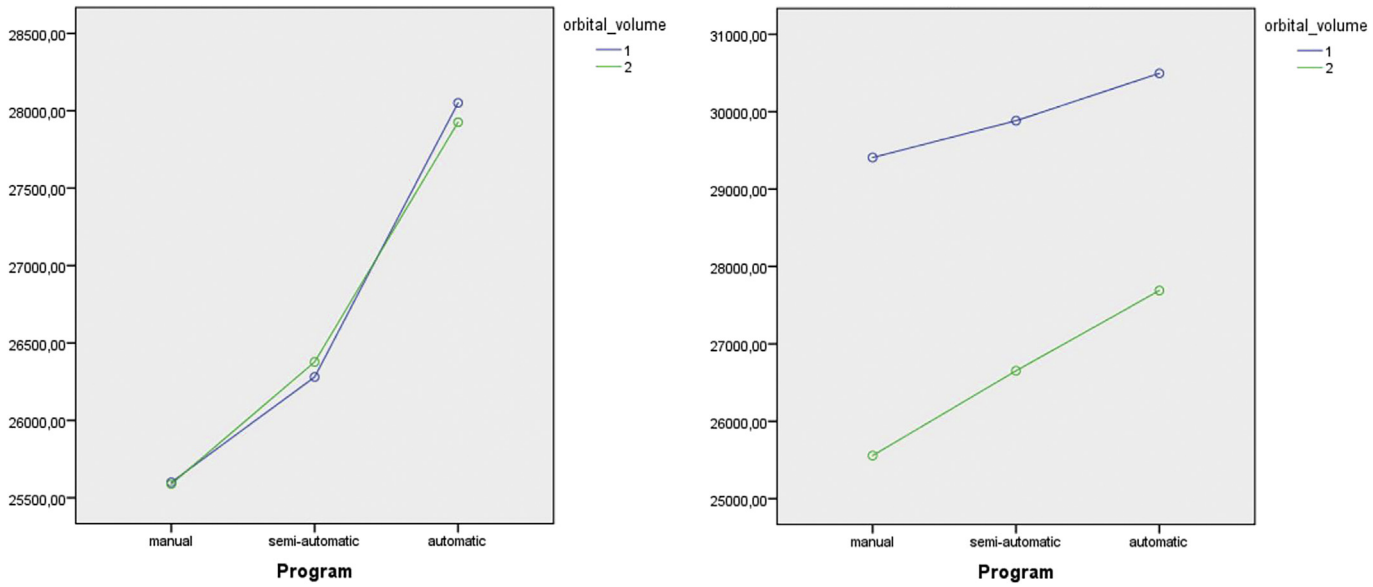

Fig. 5. Measurements of orbital volume before (1) and after (2) surgery by different methods of segmentation: a, intact orbit; b, damaged orbit.

Table 2
Volume measurements of damaged orbits.

Mode Mean volume (cm^3)	Manual	Semi-automated	Automated	p Value
Before surgery	29.4 ± 4.5	29.9 ± 4.1	30.8 ± 4.3	$p < 0.001$
After surgery	25.6 ± 3.2	26.7 ± 3.0	27.6 ± 2.9	$p < 0.001$
p Value	$p < 0.001$	$p < 0.001$	$p < 0.001$	-

and magnetic resonance imaging (MRI), as well as the development of software for imaging, segmentation, and surgical procedure simulations. Progress in orbital trauma surgery, with the development of new methods for computer-assisted navigation, computer-assisted surgery, and application of computer-aided design technologies has increased the demand for precision and accuracy of computer-based measurements for clinically significant parameters such as orbital volume and orbital wall area defects (Metzger et al., 2007; Regensburg et al., 2008; Choi and Kang, 2017; Kovar et al., 2017; Wilde et al., 2019).

Before the development of contemporary CT diagnostics, all of the indirect methods for orbital volume measurement (based on anthropometric analyses of plane radiography) demonstrated poor accuracy, and were not correlated with direct cadaveric skull measurements. In contrast, CT-based estimates of orbital volumes have been reported to correspond well with direct orbital volumetry (Cooper, 1985; Osaki et al., 2013; Diaconu et al., 2017). According to Cooper (1985), the discrepancies constituted only from 0.2% to 4%, depending on the techniques and CT quality. More recent studies by Diaconu et al. (2017) have supported this conclusion by showing no differences between direct bony orbit and eye globe volume measurements, and their evaluations by CT. At the same time, the precision of CT-based orbital volume measurements in clinical practice can be significantly lower due to anatomical conditions, CT quality, the segmentation algorithm used, and the evaluator's experience (Essig et al., 2013; Osaki et al., 2013).

Currently, several methods for CT data segmentation are available, and software programs using these methods for orbital volume measurement are available on the market (Regensburg et al., 2008; Scolozzi and Jaques, 2009; Kwon et al., 2010; Essig et al., 2013; Nilsson et al., 2018). The main user parameters that determine the software's clinical efficacy are precision, reproducibility of results, simplicity of the segmentation/modeling process, and the time required for processing.

Manual segmentation is a standard method that is often used in research as a control for evaluating errors of other segmentation techniques. It is precise and sensitive, but it is also highly time consuming and observer dependent (Jansen et al., 2016; Wagner et al., 2016). To simplify the segmentation procedure, automated or semi-automated modes of segmentation were developed. Optimization of the mathematical algorithms to locate and assess anatomical structures and their boundaries from CT data sets contributed to increased accuracy of orbital volume measurements in these automated or semi-automated modes (Paiement et al., 2014; Jansen et al., 2016; Wagner et al., 2016). Jansen et al. (2015) compared the discrepancies in orbital volume measurements using different segmentation methods and noted that semi-automated methods could be highly beneficial in clinical practice.

Table 3
Volume measurements of intact orbits.

Mode	Manual	Semi-automated	Automated	p Value
Volume difference (intact orbit before/after), cm^3	0.5 ± 0.3	0.3 ± 0.2	0.25 ± 0.15	$p = 0.75$
Volume difference (damaged orbit before/after), cm^3	3.9 ± 2.2	3.4 ± 1.6	3.2 ± 3.1	$p = 0.449$
Volume difference (intact/damaged before surgery), cm^3	3.8 ± 2.6	3.7 ± 2.2	2.8 ± 2.9	$p = 0.061$
Volume difference (intact/damaged after surgery), cm^3	0.5 ± 0.3	0.5 ± 0.4	0.76 ± 0.5	$p = 0.216$
Prolapsed soft tissue volume, cm^3	3.0 ± 1.9	3.0 ± 2.3	2.8 ± 3.9	$p = 0.152$
Orbital wall defect area, cm^2	4.7 ± 2.8	4.75 ± 3.1	4.9 ± 3.3	$p = 0.674$

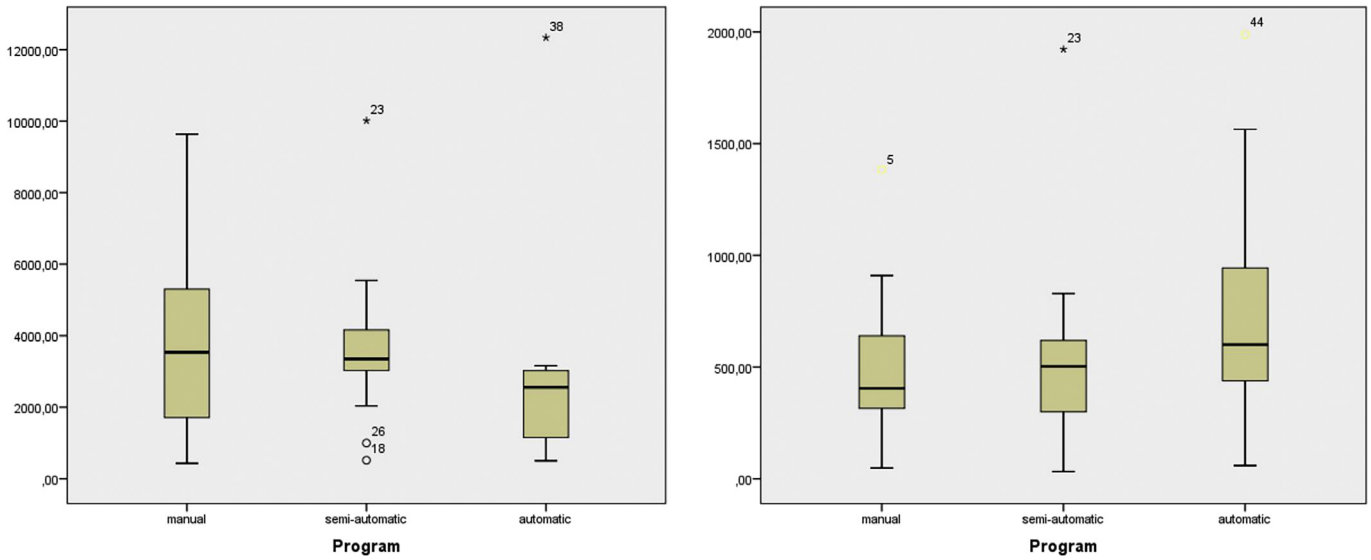

Fig. 6. Measurement of orbital-volume difference between damaged and intact orbits by different methods of segmentation: 1, before surgery; 2, after surgery.

The main factors influencing a final orbital volume value include the choice of CT or MRI, CT quality, detection of orbital boundaries, type of imaging slice (coronal or axial) selected for the evaluation, and creation of an anterior orbital surface (Kwon et al., 2010; Osaki et al., 2013; Essig et al., 2013; Wagner et al., 2016). Problems associated with these factors have not yet been solved. There are different approaches to minimize their negative effects by using different software products. Existing methods for semi-automated and automated segmentation have proved to be adequate for orbital volume measurements of intact orbits. However, in cases of orbital trauma where orbital wall defects occur, important anatomical landmarks (including the bony structures of the anterior orbital margin and the posterior orbit) are displaced or totally destroyed, and the efficacy of existing algorithms still requires validation due to possible errors in orbital volume measurements (Essig et al., 2013; Jansen et al., 2016). Most studies that compared orbital volume measurement methods were performed on cadaveric skulls or in patients with intact orbits (Regensburg et al., 2008; Jansen et al., 2016; Wagner et al., 2016).

The present study was undertaken to compare the efficacy of the most common methods for orbital volume measurement using different software programmes. We evaluated orbital trauma patterns, identified the strengths and weaknesses of each program, and made clinical recommendations for the application of existing orbital segmentation. For all of the methods, measurements of intact orbits before and after surgery showed no significant differences, with maximum deviation of less than 1 cm^3 in all cases. This provides strong evidence for the reproducibility of results obtained for all of the evaluated segmentation algorithms. The highest variability for this parameter, as well as the highest interobserver variability, was found when manual segmentation was used. This indicates the possible influence of subjective factors in this method, which a number of authors have reported to be highly observer-dependent (Essig et al., 2013; Wagner et al., 2016; Jansen et al., 2016).

At the same time, these different methods showed significant differences in orbital volume values between intact and injured orbits. Comparisons of the models derived from the different algorithm segmentations revealed that the main reason for these discrepancies was a different location of anterior orbital closing determined by each method. Even the manual and semi-automated modes, in which the approach to anterior border determination was virtually the same, showed significant differences (Fig. 7).

The problem of adequately representing the anterior orbital border is well documented in the literature, and there is no consensus for a standard method or mathematical algorithm to determine it (Osaki et al., 2013; Wagner et al., 2016). A number of authors have identified the irregular anterior orbital boundary as a source of potential error. Studies have defined this orbital boundary by a line joining the zygomaticofrontal processes, by a straight line between the medial and lateral orbital rims, or by the plane placed at the most anterior point of the lateral orbital wall (Whitehouse et al., 1994; Schuknecht et al., 1996; Essig et al., 2013; Wagner et al., 2016). However, the real orbital entrance contains no single straight line across any diameter, and using direct measurements of cadaveric orbits, their shape was determined to be convex rather than flat (Osaki et al., 2013). Therefore, the above-mentioned approaches (as well as the algorithms for manual and semi-automated segmentation in the present study) clearly exclude a portion of the anterior orbit and cause an error in volume measurement.

At the same time, all of the segmentation methods showed no differences in orbital volume changes resulting from trauma and surgical intervention, defect area, and prolapsed orbital soft tissue

Table 4
Intraobserver and interobserver intraclass correlation coefficients (ICCs) for all modes of segmentation.

Orbit	Mode	Manual	Semi-automated	Automated
Intact	Intraobserver ICC	0.988 (95% CI 0.982–0.995)	0.979 (95% CI 0.976–0.983)	0.992 (95% CI 0.987–0.997)
	Interobserver ICC	0.973 (95% CI 0.966–0.982)	0.985 (95% CI 0.981–0.993)	0.989 (95% CI 0.983–0.993)
Damaged	Intraobserver ICC	0.978 (95% CI 0.971–0.991)	0.969 (95% CI 0.959–0.981)	0.981 (95% CI 0.967–0.995)
	Interobserver ICC	0.968 (95% CI 0.957–0.979)	0.976 (95% CI 0.967–0.984)	0.979 (95% CI 0.971–0.990)

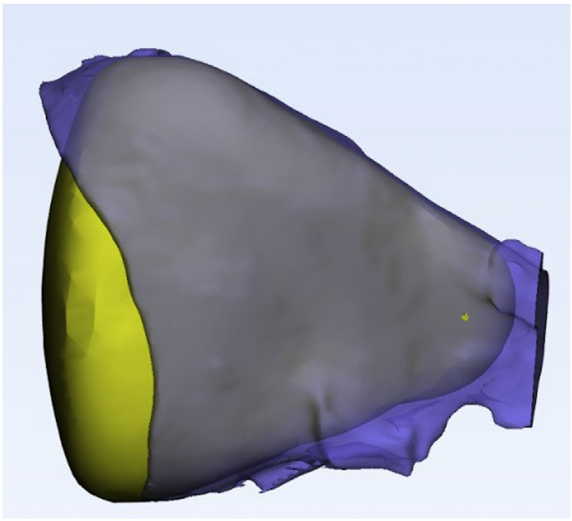

Fig. 7. Superimposition of manual (violet) and automated (yellow) orbital models of the same orbit with determination of the anterior orbital plane.

volume. These parameters are more clinically significant because they are directly related to enophthalmos and to functional deficits in orbital trauma patients (Whitehouse et al., 1994; Raskin et al., 1998; Dubois et al., 2015). The present results provide strong evidence that the precision of automated or semi-automated algorithms in modern software for determining orbital volume is virtually the same as in manual slice-by-slice segmentation. Manual segmentation proved to be more sensitive than automatic segmentation in cases of severely damaged orbits. However, in these patients, differences in injured-orbit volumes before and after reconstruction were insignificant when both the manual and automated methods of segmentation were used.

Overall, our results demonstrate that the precision and reproducibility of contemporary semi-automated and automated (model-based) methods using in D2P and Disior Orbital Analysis Software did not differ significantly from these same parameters using standard manual segmentation. These methods proved to be reliable, less observer-dependent, and much less time-consuming when compared to manual segmentation.

Within a method, orbital volume change values after trauma or surgical interventions matched, but across methods, absolute orbital volume values were significantly different. In view of this, results obtained by different methods and in different studies should be compared using only relative changes in orbital volume, and not using absolute orbital volume values. In clinical practice, it is important that the same segmentation method be used before and after surgery. The choice of method depends mainly on the available software, and the evaluator's experience and preferences. In our experience, automated segmentation has the significant benefits of simplicity, predictability, and less time involvement.

5. Conclusions

Our results demonstrated, that the analyzed segmentation methods had the same accuracy in evaluation of volume differences between two orbit of the same patient, defect areas, and prolapsed soft-tissue volumes but not in absolute values of the orbital volume due to the existing diversity in determination of anterior closing. The automated method is recommended for common clinical cases, as les time-consuming with high precision and reproducibility.

Declaration of Competing Interest

The authors declare that they have no conflicts of interest.

Acknowledgements

The authors thanks the “Imatek Medical Co” and Disior Ltd for technical support in this study.

References

Bijlsma WR, Mourits MP: Radiologic measurement of extraocular muscle volumes in patients with graves' orbitopathy: a review and guideline. Orbit 25(2): 83–91. https://doi.org/10.1080/01676830600675319, 2006

Choi S, Kang D: Prediction of late enophthalmos using preoperative orbital volume and fracture area measurements in blowout fracture. J Craniofac Surg 7(28): 1717–1720. https://doi.org/10.1097/SCS.0000000000003765, 2017

Comerci M, Elefante A, Strianese D, Senese R, Bonavolontà P, Alfano B, et al: Semiautomatic regional segmentation to measure orbital fat volumes in thyroid-associated ophthalmopathy a validation study. Neuroradiol J 26(4): 373–379. https://doi.org/10.1177/197140091302600402, 2013

Cooper WC: A method for volume determination of the orbit and its contents by high-resolution axial tomography and quantitative digital image analysis. Trans Am Ophthalmol Soc 83: 546–609, 1985

Diaconu S, Dreizin D, Uluer M, Mossop C, Grant MP, Nam AJ: The validity and reliability of computed tomography orbital volume measurements. J Craniofac Surg 45(9): 1552–1557. https://doi.org/10.1016/j.jcms.2017.06.024, 2017

Dubois L, Steenen S, Gooris P, Mourits M, Becking A: Controversies in orbital reconstruction—I. Defect-driven orbital reconstruction: a systematic review. Int J Oral Maxillofac Surg 44(3): 308–315. https://doi.org/10.1016/j.ijom.2014.12.002, 2015 Epub 2014 Dec 24

Essig H, Dressel L, Rana M, Kokemueller H, Ruecker M, Gellrich NC: Precision of posttraumatic primary orbital reconstruction using individually bent titanium mesh with and without navigation: a retrospective study. Head Face Med 2: 9–18. https://doi.org/10.1186/1746-160X-9-18, 2013

Fu Y, Liu S, Li H, Yang D: Automatic and hierarchical segmentation of the human skeleton in CT images. Phys Med Biol 62(7): 2812–2833. https://doi.org/10.1088/1361-6560/aa6055, 2017

Galibourg A, Dumoncel J, Telmon N, Calvet A, Michetti J, Maret D: Assessment of automatic segmentation of teeth using a watershed-based method. Dentomaxillofacial Radiol 47: 20170220. https://doi.org/10.1259/dmfr.20170220, 2018

Hu YC, Grossberg MD, Wu A, Riaz N, Perez C, Mageras GS: Interactive semiautomatic contour delineation using statistical conditional random fields framework. Med Phys 39(7): 4547–4558. https://doi.org/10.1118/1.4728979, 2012

Jansen J, Schreurs R, Dubois L, Maal TJ, Gooris PJ, Becking AG: Orbital volume analysis: validation of a semi-automatic software segmentation method. Int J Comput Assist Radiol Surg 11(1): 11–18. https://doi.org/10.1007/s11548-015-1254-6, 2016 Epub 2015 Jul 16

Kärkkäinen M, Wilkmanb T, Mesimäki K, Snäll J: Primary reconstruction of orbital fractures using patient-specific titanium milled implants: the Helsinki protocol. Br J Oral Maxillofac Surg 56(9): 791–796. https://doi.org/10.1016/j.bjoms.2018.08.008, 2018 Epub 2018 Sep. 13

Kovar D, Voldrich Z, Voska P, Lestak J, Astl J: Indications for repositioning of blowout fractures of the orbital floor based on new objective criteria—tissue protrusion volumometry. Biomed Pap Med Fac Palacky Univ Olomouc Czech Repub 161(4): 403–406. https://doi.org/10.5507/bp.2017.036, 2017 Epub 2017 Aug 31

Kwon L, Barrera J, Most S: Comparative computation of orbital volume from axial and coronal CT using three-dimensional image analysis. Ophthalmic Plast Reconstr Surg 26: 26–29. https://doi.org/10.1097/IOP.0b013e3181b80c6a, 2010

Lukats O, Vízkelety T, Markella Z, Maka E, Kiss M, et al: Measurement of orbital volume after enucleation and orbital implantation. PLoS One 7(12): e50333. https://doi.org/10.1371/journal.pone.0050333, 2013

Metzger MC, Bittermann G, Dannenberg L, Schmelzeisen R, Gellrich NC, Hohlweg-Majert B, et al: Design and development of a virtual anatomic atlas of the human skull for automatic segmentation in computer-assisted surgery, preoperative planning, and navigation. Int J Comput Assist Radiol Surg 8(5): 691–702. https://doi.org/10.1007/s11548-013-0818-6, 2013

Metzger MC, Hohlweg-Majert B, Schön R, Teschner M, Gellrich NC, Schmelzeisen R, et al: Verification of clinical precision after computer-aided reconstruction in craniomaxillofacial surgery. Oral Surg Oral Med Oral Pathol Oral Radiol Endod 104: e1–e10. https://doi.org/10.1016/j.tripleo.2007.04.015, 2007

Nilsson J, Nysjö J, Carlsson A-P, Thor A: Comparison analysis of orbital shape and volume in unilateral fractured orbits. J Cranio-Maxillo-Fac Surg 46(3): 381–387. https://doi.org/10.1016/j.jcms.2017.12.012, 2018

Noser H, Hammer B, Kamer L: A method for assessing 3D shape variations of fuzzy regions and its application on human bony orbits. J Digit Imag 23: 422–429, 2018

Osaki T, de Castro D, Yabumoto C, Mingkwansook V, Ting E, Nallasamay N, et al: Comparison of methodologies in volumetric orbitometry. Ophthalmic Plast Reconstr Surg 29: 431–436, 2013

Paiement A, Mirmehdi M, Xianghua X, Hamilton M: Integrated segmentation and interpolation of sparse data. IEEE Trans Image Proc 23(1): 110–125. https://doi.org/10.1109/tip.2013.2286903, 2014

Queiroz P, Rovaris K, Santaella G, Haiter-Neto F, Freitas D: Comparison of automatic and visual methods used for image segmentation in endodontics: a microCT study. J Appl Oral Sci 25(6): 674–679. https://doi.org/10.1590/1678-7757-2017-0023, 2017

Raskin E, Millman A, Lubkin V, della Rocca R, Lisman R, Maher E: Prediction of late enophthalmos by volumetric analysis of orbital fractures. Ophthalmic Plast Reconstr Surg 14: 19–26, 1998

Regensburg N, Kok P, Zonneveld F, Baldeschi L, Saeed P, Wiersinga W, et al: A new and validated CT-based method for the calculation of orbital soft tissue volumes. Invest Ophthalmol Vis Sci 49: 1758–1762. https://doi.org/10.1167/iovs.07-1030, 2008

Scolozzi P, Jaques B: Computer-aided volume measurement of posttraumatic orbits reconstructed with AO titanium mesh plates: accuracy and reliability. Ophthalmic Plast Reconstr Surg 24(5): 383–389. https://doi.org/10.1097/IOP.0b013e318185a72c, 2008

Sozzi D, Gibelli D, Canzi G, Tagliaferri A, Monticelli L, Cappella A, et al: Assessing the precision of posttraumatic orbital reconstruction through “mirror” orbital superimposition: a novel approach for testing the anatomical accuracy. J Craniomaxillofac Surg 46(8): 1258–1262. https://doi.org/10.1016/j.jcms.2018.05.040, 2018

Strong E, Fuller S, Chahal H: Computer-aided analysis of orbital volume: a novel technique. Ophthalmic Plast Reconstr Surg 29(1): 1–5. https://doi.org/10.1097/IOP.0b013e31826a24ea, 2013

Schuknecht B, Carls F, Valavanis A, Sailer H: CT assessment of orbital volume in late post-traumatic enophthalmos. Neuroradiology 38(5): 470–475, 1996

Tang X, Liu H, Chen L, Wang Q, Luo B, Xiang N, et al: Semi-automatic volume measurement for orbital fat and total extraocular muscles based on Cube FSE-flex sequence in patients with thyroid-associated ophthalmopathy. Clin Radiol 73(8): 759.e11–759.e17. https://doi.org/10.1016/j.crad.2018.02.011, 2018

Wagner M, Gellrich N, Friese K, Becker M, Wolter F, Lichtenstein J, Stoetzer M, Rana M, Essig H: Model-based segmentation in orbital volume measurement with cone beam computed tomography and evaluation against current concepts. Int J Comput Assist Radiol Surg 11(1): 1–9. https://doi.org/10.1007/s11548-015-1228-8, 2016 Epub 2015 Jun 5

Whitehouse R, Batterbury M, Jackson A, Noble J: Prediction of enophthalmos by computed tomography after “blow out” orbital fracture. Br J Ophthalmol 78: 618–620, 1994

Wilde F, Krauß O, Sakkas A, Mascha F, Pietzka S, Schramm A: Custom wave-shaped CAD/CAM orbital wall implants for the management of post-enucleation socket syndrome. J Craniomaxillofac Surg 47(9): 1398–1405. https://doi.org/10.1016/j.jcms.2019.06.015, 2019